Mnd1p: An evolutionarily conserved protein required for meiotic recombination

Jennifer L. Gerton and Joseph L. DeRisi*

Department of Biochemistry and Biophysics, University of California, 513 Parnassus Avenue, Box 0448, San Francisco, CA 94143-0448

Communicated by Thomas D. Petes, University of North Carolina, Chapel Hill, NC, March 22, 2002 (received for review February 21, 2002)

We used a functional genomics approach to identify a gene required for meiotic recombination, YGL183c or *MND1*. *MND1* was spliced in meiotic cells, extending the annotated YGL183c ORF N terminus by 45 aa. *Saccharomyces cerevisiae mnd1–1* mutants, in which the majority of the *MND1* coding sequence was removed, arrested before the first meiotic division with a phenotype reminiscent of *dmc1* mutants. Physical and genetic analysis showed that these cells initiated recombination, but did not form heteroduplex DNA or double Holliday junctions, suggesting that Mnd1p is involved in strand invasion. Orthologs of *MND1* were identified in protists, several yeasts, plants, and mammals, suggesting that its function has been conserved throughout evolution.

Sexually reproducing organisms have a specialized developmental pathway for gametogenesis in which diploid cells undergo meiosis to produce haploid germ cells. Before the first meiotic division, while cells contain replicated pairs of homologs, recombination occurs. The process of recombination serves at least three purposes: (*i*) to provide an opportunity for damage to homologs to be repaired, (*ii*) to generate diversity, and (*iii*) to facilitate proper chromosome segregation.

Meiotic recombination in *Saccharomyces cerevisiae* is initiated by double-strand breaks (DSBs) made by the Spo11p endonuclease (1, 2). The 5′ ends of these breaks are then resected (3) in a process involving *RAD50/MRE11*. Several genes, including *RAD51* and *DMC1*, promote invasion of the homologous chromosome by a 3′ single-stranded DNA end. After DNA synthesis, second-end capture, and ligation, double Holliday junctions or joint molecules (JMs) that contain heteroduplex DNA (hDNA) are formed (4, 5). For each JM, resolution is required for the completion of recombination and proper chromosome separation at the first meiotic division. In the original DSB repair model, crossover (CO) and noncrossover (NCO) recombinants are proposed to be alternatively resolved products of a single intermediate JM species (6). However, recent kinetic evidence suggests that CO and NCO products can be produced from different intermediates (7).

Using a functional genomics approach, we identified a meiosis-specific protein in *S. cerevisiae* that is required for recombination. The gene encoding this activity is YGL183c, or *MND1* [Meiotic Nuclear Divisions (8)]. Sequence of the cDNA corresponding to *MND1* revealed that the meiotic transcript was spliced, yielding a coding sequence 45 aa longer than the annotated YGL183c ORF. *mnd1–1* mutants in which base pairs 136–661 of correct *MND1* gene sequence had been deleted arrested before the first meiotic division. These cells initiated recombination but did not form hDNA or JMs. Our results suggest that Mnd1p is required for stable hDNA formation. We identified orthologs of *MND1* in protists, several yeasts, *Arabidopsis thaliana*, *Mus musculus*, and *Homo sapiens*, suggesting that the function of Mnd1p has been conserved throughout two billion years of evolution.

Materials and Methods

Strains. The plasmid for replacement of base pairs 136–661 of YGL183c with the gene for kanamycin resistance was obtained from the Eurofan I deletion project at the Institute for Microbiology at Johann Wolfgang Goethe-University Frankfurt, Frankfurt. This mutation is referred to as *mnd1–1*. KBY80 (*leu2*::*hisG*/*leu2*::*hisG* ho::*LYS2 lys2*/*lys2*, *ura3*/*ura3*) was the wild-type (wt) diploid SK1 strain used for assaying nuclear division. JG702 and JG802 are isogenic with KBY80 with *mnd1–1*::kan^r/*mnd1–1*::kan^r and *dmc1*::*LEU2*/*dmc1*::*LEU2*, respectively. JG721, JG710, and JG709 are all isogenic to JG702 with *spo11*::*URA3*/*spo11*::*URA3*,*spo13*::*hisG*/*spo13*::*hisG*, and *rad17*::*hisG-URA3*/*rad17*::*hisG-URA3*, respectively. For measuring heteroallele recombination in the SK1 background, the wt diploid strain JG751 was used (*arg4-Nsp*/*arg4-Bgl his4-B*/*his4-X leu2*/*leu2 trp1*/*trp1 ura3*/*ura3*) (9). JG750 is isogenic to JG751 with *mnd1–1*::kan^r/*mnd1–1*::kan^r. For the physical analysis of DSBs at *HIS4* in S288c, the diploid wt strain QFY105 was used (*trp1*/*TRP1 arg4*/*ARG4 tyr7*/*TYR7 ade6*/*ade6 ura3*/*ura3 LEU2*/*leu2 HIS4*/*his4-IR9 rad50S-URA3*/*rad50S-URA3*) (10). JG166 is isogenic to QFY105 except for the *HIS4* gene (*HIS4*/*his4-AAG*) (11) and *mnd1–1*::kan^r/*mnd1–1*::kan^r. For the physical analysis of hDNA at *HIS4* in S288c, the diploid wt strain DNY86 was used (*trp1*/*TRP1 arg4*/*ARG4 tyr7*/*TYR7 ade6*/*ade6 ura3*/*ura3 LEU2*/*leu2 his4-IR15*/*his4-IR16*) (12). JG190 is isogenic to DNY86 with *mnd1–1*::kan^r/*mnd1–1*::kan^r. For measuring heteroallele recombination in S288c, the wt diploid strain used was MS1. This strain is isogenic with DNY86 with the exception of the *HIS4* locus (*his4–713*/*his4-Sal)* (12). JG197 is isogenic with *mnd1–1*::kan^r/*mnd1–1*::kan^r. For the analysis of DSBs, COs, and JMs in SK1, we used MJL2442 (7). JG774, JG820, and JG819 are all isogenic to MJL2442 with *mnd1–1*::kan^r/*mnd1–1*::kan^r, *dmc1*::*LEU2*/*dmc1*::*ARG4*, or both, respectively.

Sporulation Conditions. For S288c strains, cultures grown in YPD (1% yeast extract, 2% peptone, 2% dextrose) overnight at 30°C were diluted into SPS (0.5% yeast extract, 1.0% peptone, 0.17% yeast nitrogen base, 1.0% KOAc, 0.5% ammonium sulfate, 0.05 M potassium phthalate) to OD_{600} = 0.2 and shaken for 18–20 h at 30°C. Cells were collected by centrifugation, washed once with 1% KOAc, and then resuspended in the same volume of 1% KOAc as the SPS culture. Cultures were shaken at room temperature and aliquots were removed at the indicated times. For SK1 strains, YPD overnight cultures were diluted into YPA (1% KOAc, 2% peptone, 1% yeast extract) to OD_{600} = 0.2 and shaken for 14–16 h at 30°C. Cells were collected by centrifugation, washed once with SPM (1% KOAc, 0.02% raffinose), and then resuspended in the same volume of SPM as the YPA culture. Cultures were shaken at 30°C and aliquots were removed at the indicated times. For assaying nuclear division, formaldehyde was added to 4.5% for at least 1 h before proceeding with the staining protocol. For return-to-growth experiments, cells were diluted and plated on synthetic dextrose (SD) complete

Abbreviations: hDNA, heteroduplex DNA; JM, joint molecule; CO, crossover; NCO, noncrossover; DSB, double-strand break; wt, wild type; SD, synthetic dextrose; DAPI, 4′,6-diamindine-2-phenylindole; 1D, one-dimensional; 2D, two-dimensional.

*To whom reprint requests should be addressed. E-mail: joe@derisilab.ucsf.edu.

The publication costs of this article were defrayed in part by page charge payment. This article must therefore be hereby marked "*advertisement*" in accordance with 18 U.S.C. §1734 solely to indicate this fact.

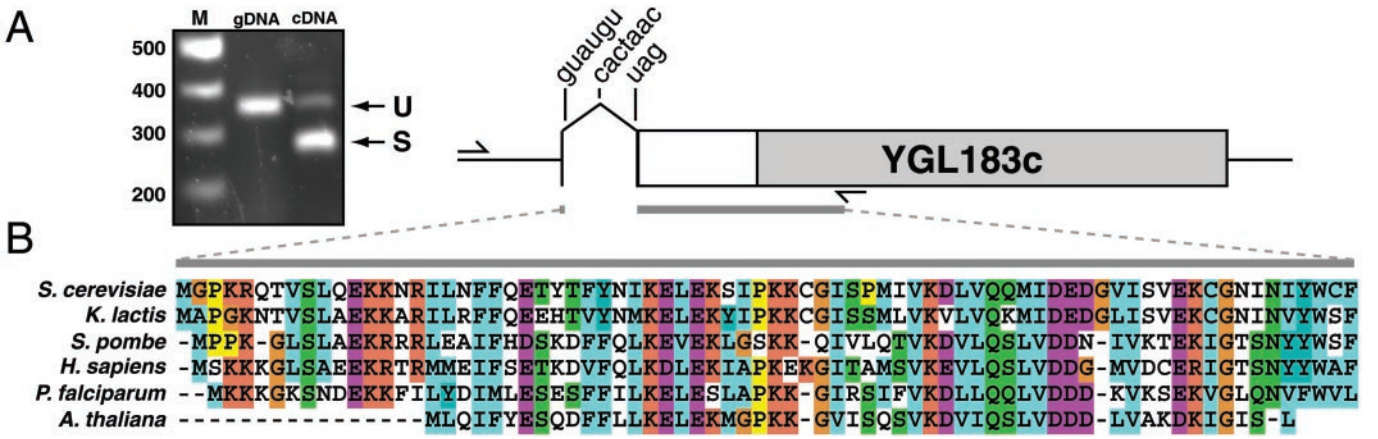

Fig. 1. Mnd1 was spliced in meiotic cells. (*A*) PCR amplification from genomic DNA and cDNA reveals a spliced transcript in meiotic cells. U indicates unspliced, and S indicates spliced. In the diagram at the right, the 5′ and 3′ splice and branchpoint sequences and PCR primers are indicated. The white box shows the extension of the reading frame for YGL183c in the 5′ direction. The gray bars correspond to the region for which an alignment is shown in *B*. (*B*) CLUSTALX was used to align N termini of predicted orthologous *Mnd1* genes from *S. cerevisiae*, *K. lactis*, *S. pombe*, *H. sapiens*, *P. falciparum*, and *A. thaliana*.

medium to monitor cell viability or on SD medium lacking histidine or arginine to detect recombination. For preparation of RNA and DNA, cells were collected by centrifugation, frozen in liquid nitrogen, and stored at −80°C until processed further.

Assaying for Nuclear Division. After incubation in formaldehyde, cells were washed twice in PBS, resuspended in 1 μg/ml 4′,6-diamindine-2-phenylindole (DAPI) in PBS, and incubated for 12 min in the dark. Cells were washed twice with PBS, resuspended in PBS, and imaged with an Olympus BX60 fluorescence microscope.

DNA Preparation. For one-dimensional (1D) gels, genomic DNA was prepared essentially as described (12), with the addition of a phenol:chloroform extraction before the final ethanol precipitation. For two-dimensional (2D) gels, genomic DNA was prepared exactly as described (13).

RNA and cDNA Preparation. Poly(A)$^+$ RNA from KBY80 at 6 h in sporulation was prepared as described (14). Reverse transcription was carried out with 400 ng of poly(A)$^+$ RNA and primer 1 (5′-ACCACATTTTTCCACCGAA). The resulting cDNA was used as a template in a PCR containing primer 1 and primer 2 (5′-CCACCGTTATTCTTTGCGAT).

Southern Blotting. Standard Southern blotting protocols were used (15). Visualization and quantitation of bands was accomplished with a PhosphorImager and IMAGEQUANT software. The probe for the Southern blot found in Fig. 4 *B* and *C* was a PCR fragment from *HIS4* (SGD coordinates 66663–68236 for chromosome III). The probe used in Fig. 5*B* was a PCR fragment from *ARG4* (*Saccharomyces* Genome Database coordinates 140119–141267 for chromosome VIII). These DNA fragments were radiolabeled by using standard random hexamer labeling with exo-free Klenow and α-^{32}P-dCTP (15).

2D Native/Native Gels. Methods used were exactly as described (7).

Results

Identification of Genes Involved in Meiotic Recombination. A transcriptional profile of the meiotic process reveals four main categories of induction: (*i*) metabolic genes induced by nitrogen starvation, (*ii*) early (I and II) genes that include genes involved in synapsis of homologous chromosomes and recombination, (*iii*) middle genes, which are involved in processes such as the mechanics of meiotic division and spore morphogenesis, and (*iv*) late genes, which are mostly involved in spore wall formation (14). Of the 32 genes in the early I cluster, more than half have been shown to have sporulation defects. To identify genes involved in meiotic recombination, we constructed deletions of 12 genes in the early I cluster that had uncharacterized phenotypes in meiosis and analyzed the ability of these mutants to form tetrads (Table 1, which is published as supporting information on the PNAS web site, www.pnas.org). Of these 12, YOR177c and YGL183c were the only genes essential for tetrad formation. YOR177c has since been named *MPC54* and is a meiosis-specific component of the spindle pole body (16). YGL183c has been named *MND1*; mutants have been shown to arrest before the first meiotic division (ref. 8, see Fig. 2*A*).

***MND1* Does Not Play a Role in Mitotic DNA Metabolism.** *MND1* was disrupted in the Eurofan 1 project and analyzed for defects in DNA metabolism and meiosis. Specifically, the mutant strain was assayed for DNA damage response, UV sensitivity, gamma ray sensitivity, mitotic mutation rate in the *CAN1* gene, mitotic recombination between direct and inverted repeats, hydroxyurea sensitivity, and ability to sporulate. In all cases but sporulation, the *mnd1–1* mutation had no effect (http://mips.gsf.de/proj/eurofan/eurofan_2.html). Transcription of this gene is not induced under any of the 300 growth conditions that have been examined in yeast except for sporulation (http://www.transcriptome.ens.fr/ymgv), suggesting that this gene is only involved in processes that occur during sporulation.

***MND1* Was Spliced During Meiosis.** The predicted ORF for *MND1* can be extended at the 5′ end by homology to orthologs of *MND1* in other organisms (17). When 132 bp upstream of the annotated YGL183c ORF are translated, the resulting peptide sequence is 36% identical to the N terminus of the orthologous human protein. This region does not contain any stop codons and is in-frame with the rest of the gene, yet it does not contain a Met start codon, as confirmed by sequencing genomic DNA. However, sequence of the predominant form of the cDNA in meiotic cells (Fig. 1*A*) revealed a spliced transcript in which an 83-bp intron extends the N terminus of the annotated YGL183c ORF by 45 aa. The *MND1* intron contains a 5′ consensus splice site (GUAUGU), a 3′ consensus splice site (CAG), and a noncanonical branch point (cACUAAC) (Fig. 1*A*).

Orthologs of *MND1* Exist in Several Fungi, Protists, Plants, and Animals. We found orthologs of *MND1* in the hemiascomycetous yeasts *Saccharomyces byanus* (79% identity), *Saccharomyces*

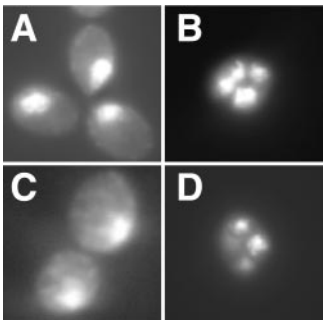

Fig. 2. Nuclear division. Cells were collected at 11 h postintroduction into sporulation media, stained with DAPI, and photographed. (*A*) *mnd1–1*; (*B*) *mnd1–1spo11*; (*C*) *mnd1–1spo13*; and (*D*) *mnd 1–1rad17*. (Magnifications: ×100.)

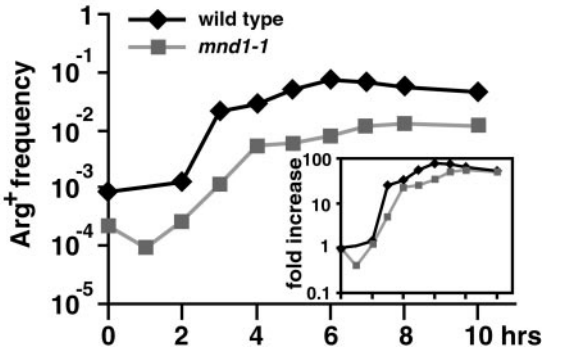

Fig. 3. Heteroallele recombination at *ARG4* in SK1. JG750 (*mnd1–1*) and JG751 (wt) were put into sporulation media at time 0 h, and aliquots were removed and plated on SD-complete or SD-arginine at indicated times. Data points were the average measurement from two independent isolates.

kluyveri (82% identity), *Kluyveromyces thermotolerans* (37% identity), *Kluyveromyces lactis* (31% identity), *Debaryomyces hansenii* (43% identity), in *Schizosaccharomyces pombe* (21% identity), in the plant *A. thaliana* (14% identity), in the protists *Encephalitozoon cuniculi* (21% identity), *Giardia lamblia* (22% identity), and *Plasmodium falciparum* (15% identity), and in the mammals mouse (23% identity) and human (24% identity). Notably, we were unable to identify orthologs of *MND1* in *Caenorhabditis elegans* or *Drosophila melanogaster*. The alignment among the N termini of proteins (Fig. 1*B*) revealed a very highly conserved region that does not have a significant match to any known functional domain. Amino acids 118–139 encode a putative nuclear localization signal (18).

***MND1* Functions After DSB Formation.** *mnd1–1* mutants in the SK1 strain background arrested before the first meiotic division (Fig. 2*A*). To further dissect the role of *MND1*, we explored the phenotype of an *mnd1–1* mutant in combination with null mutations in (*i*) *SPO11*, which makes DSBs, (*ii*) *SPO13*, which causes a single MII-like division (19), and (*iii*) *RAD17*, a checkpoint gene that detects unresolved recombination intermediates (20). Each of these double mutants was sporulated and DNA was stained with DAPI. In the *mnd1–1spo11* mutant, tetrads were formed with wt efficiency (Fig. 2*B*), as they are in a *spo11* mutant, but the spores were not viable (0/40 spores from 10 dissected tetrads grew), presumably caused by the massive chromosome segregation defects observed in spores in *spo11* mutants (21). Deletion of *SPO13* results in viable dyads when combined with a mutation that blocks the initiation of recombination (e.g., a *SPO11* deletion). In *mnd1–1spo13*, the cells arrested with one DAPI-staining body (Fig. 2*C*). This result indicates that *MND1* operates after DSB formation. These results are consistent with a previous report that shows that in a *spo11spo13* background an *mnd1–1* mutant can form some viable spores in dyads (8). Finally, in the *mnd1–1 rad17* mutant, meiotic divisions occurred and four DAPI-staining bodies were produced (Fig. 2*D*), but mature spores were not formed. This finding indicates that the arrest in an *mnd1–1* strain was caused by the *RAD17*-mediated checkpoint that detects unresolved recombination intermediates.

Because spore formation was defective in the *mnd1–1* strain, we measured recombination by the return-to-growth assay, which allows for the recovery of diploid cells that have initiated meiotic recombination between heteroalleles by DSBs but are unable to repair them at later stages. Cells were withdrawn from sporulation medium and transferred to nutrient-rich medium to assess commitment to meiotic recombination (22). In general, heteroallelic recombination reflects NCO recombination, or gene conversion. However, heteroallelic recombination in a return-to-growth experiment may not require wt end resection and/or heteroduplex formation because a *dmc1* strain behaves like wt in this assay despite having hyperresected DSBs (23) and no detectable JMs (24). The average frequency of *ARG+* prototrophs at 7 h in the wt SK1 strain was 6.5×10^{-2} and 1.1×10^{-2} in an *mnd1–1* strain (Fig. 3). Because Mnd1 is not expressed during mitotic growth, the difference at time 0 h is presumably stochastic. When the difference in the baseline is adjusted, the induction of recombination is similar; the *mnd1–1* strain induced recombination an average of 49-fold and the wt strain induced recombination an average of 74-fold at the 7 h time point (see Fig. 3 *Inset*). Furthermore, the kinetics of recombination induction appeared to be similar; commitment to meiotic recombination began at about 3 h after transfer to sporulation media and leveled off by 6 h in both wt and *mnd1–1* strains. Similar results were observed at the *his4* locus (data not shown). These data suggest that *MND1* is not required for the induction of the high levels of recombination characteristic of meiosis.

***MND1* Was Required for Stable hDNA Formation.** Initiation of recombination may be directly monitored by examining DSBs. The *HIS4* promoter sequence contains a hotspot for DSB formation (Fig. 4*A*). DSBs at the *HIS4* locus in S288c-derived strains have been characterized in detail (10–12, 25). In a *rad50S* strain, the ends of DSBs are not processed, facilitating visualization by Southern blot (26). We analyzed the levels of *HIS4* DSBs formed in a *rad50S* strain in an otherwise wt strain background (QFY105) and an *mnd1–1* strain (JG166, Fig. 4*A*). At 24 h, the levels of DSBs in these strains were comparable; *rad50S* had 1.7% DSB and *rad50S mnd1–1* had 2.5% DSB. This result indicates that the level of DSBs was not diminished by mutation of *MND1*. When we measured DSBs in a *RAD50* strain background (where DSBs are processed), we observed no difference in the levels of DSBs in wt and *mnd1–1* strains (data not shown).

Nag and Petes (12) developed a physical assay to detect hDNA at the *HIS4* locus during meiotic recombination. The strain used in this assay, DNY86, contains one chromosome with a *Bam*HI site inserted into the *Sal*I site of the *HIS4* gene and a second chromosome with a *Pst*I site inserted into the same *Sal*I site in *HIS4*. hDNA will contain one DNA strand with a *Bam*HI site and one strand with a *Pst*I site and therefore will not be cut with either enzyme. hDNA first occurs post-DSB, when 3′ single-stranded DNA from the break site invades the homologous chromosome. This recombination intermediate, referred to as a single-end invasion, is relatively unstable, but can be observed if DNA is crosslinked with psoralen before extraction from cells (24). hDNA will persist in the cell in both NCO and CO recombination intermediates and products. Nag and Petes (12)

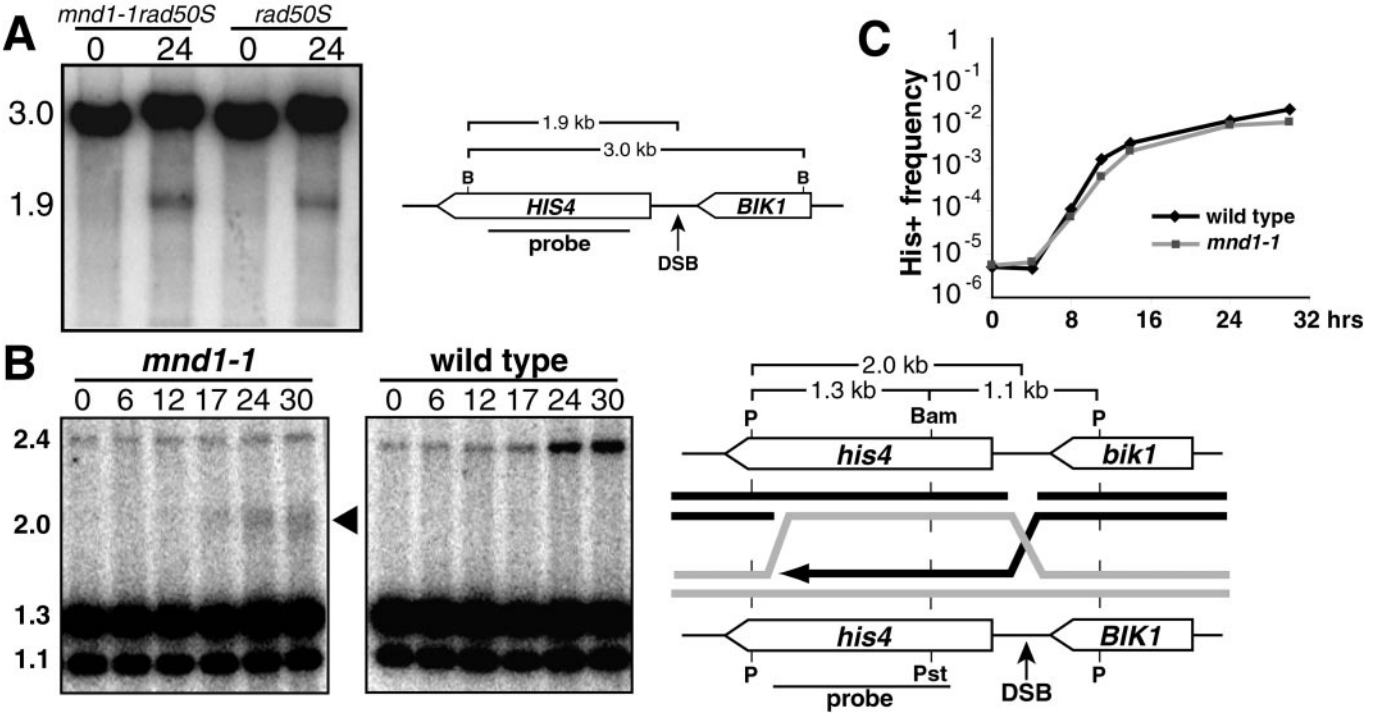

Fig. 4. Physical analysis of *HIS4* hotspot, S288c. (*A*) Genomic DNA was isolated from QFY105 (*rad50S*) and JG166 (*rad50S mnd1–1*) after 0 and 24 h in sporulation medium. DNA was digested with *Bgl*II, electrophoresed on a 0.8% agarose gel, transferred to a nylon membrane, and hybridized to a ^{32}P-labeled DNA fragment indicated as probe. The 3.0-kb fragment is the parental band and the 1.9-kb band corresponds to the DSB. (*B*) Genomic DNA was isolated from DNY86 (wt) and JG190 (*mnd1–1*) at the indicated times after transfer to sporulation medium. A 30-bp palindrome sequence containing a *Pst*I site (inserted at the *Sal*I site of *his4*) was present on one homolog of chromosome III and a 32-bp palindrome sequence containing a *Bam*HI site (inserted at the *Sal*I site of *his4*) was present on the other homolog of chromosome III. DNA was digested with *Pst*I, *Pvu*II (P), and *Bam*HI. The 1.3- and 1.1-kb bands are the parental fragments and the 2.4-kb band corresponds to hDNA. (*C*) JG197 (*mnd1–1,* squares) and MS1 (wt, diamonds) were put into sporulation media at time 0 h and aliquots were removed and plated on SD-complete or SD-histidine at indicated times. Time in hours is depicted on the *x* axis and the frequency of *HIS*+ prototrophs is shown according to the log scale on the *y* axis.

demonstrated that hDNA cannot be detected in a *rad50* strain (which cannot make DSBs), but can be detected in a *rad52* strain, which is defective in a later stage of recombination. The hDNA detected by this assay is presumably derived from both CO and NCO recombination intermediates and products.

We used this physical assay to determine whether stable hDNA formation occurred in *mnd1–1* mutants. The 2.4-kb band diagnostic of hDNA in wt was not formed in the isogenic *mnd1–1* strain (Fig. 4*B*). We always observed a background band at 2.4 kb that was meiosis independent. Although hDNA was not detected at the *his4* locus in the *mnd1–1* strain, heteroallelic recombination at this same *his4* locus in a return-to-growth assay was reduced only 2-fold in an *mnd1–1* strain and did not show any delay in recombination induction relative to the isogenic wt strain (Fig. 4*C*). Even though DSBs were plentiful in an *mnd1–1* strain, and could be used efficiently for heteroallele recombination in a return-to-growth experiment, this strain was not able to form stable hDNA.

In the Southern blot shown in Fig. 4*B*, the *mnd1–1* strain contained a band at 2.0 kb. This band most likely reflects DSBs that have 5′ ends that have been resected past the *Pst*I or *Bam*HI restriction enzyme sites (which have been inserted at the *Sal*I site, approximately 630 bp away from the DSB site); the 3′ single-stranded DNA is therefore resistant to digestion. This distance is consistent with what has been observed genetically, which is that heteroduplexes at *HIS4* often span a distance of 1.8 kb (25). Thus, in *mnd1–1* strains, 5′ end resection has occurred, and long single-stranded 3′ tails are present but unable to stably invade the homologous chromosome to form hDNA.

***MND1* Was Required to Complete CO Recombination.** We explored the status of recombination intermediates in an *mnd1–1* strain at a synthetically created hotspot in the SK1 strain background by using the procedures of Allers and Lichten (7). In brief, the *LEU2* locus on one chromosome III homolog has a cassette inserted into it that contains *URA3* and *ARG4.* The other homolog has a similar cassette inserted into the *HIS4* locus (Fig. 5*A*). These markers make it possible to monitor DSBs, COs, and JMs. Fig. 5*B* shows a Southern blot of DNA from a meiotic time series of a wt strain (MJL2442) and an *mnd1–1* strain (JG774) digested with *Xho*I. The parental fragments were 12.4 and 12.7 kb, DSBs were 3.7 and 2.4 kb, and CO products were 19.8 and 5.2 kb. DSBs appeared at 3 h after transfer to sporulation medium in both strains in the time course shown, and by 2 h in an independent time course (data not shown). However, the *mnd1–1* strain had ≈2-fold more DSBs at the 3, 4, 5, 6, and 7 h time points. We could detect the 5.2-kb CO product (the 19.8-kb CO product did not transfer well presumably because of its large size) in the wt strain by 5 h in the time course shown, and by 4 h in an independent time course. The CO product was undetectable in the *mnd1–1* strain in both time courses, even at 7 and 8 h. Thus, *MND1* was required to complete CO recombination.

***MND1* Was Required for JM Formation.** We further investigated the defect in the *mnd1–1* strain by assessing JM formation. JMs are considered to be the hDNA-containing precursors of all CO recombinants and some or all NCO recombinants (5, 7). JMs can be detected by 2D native/native gels in which the first dimension separates DNA based on mass and the second dimension separates DNA based on mass and shape. The bulk of genomic

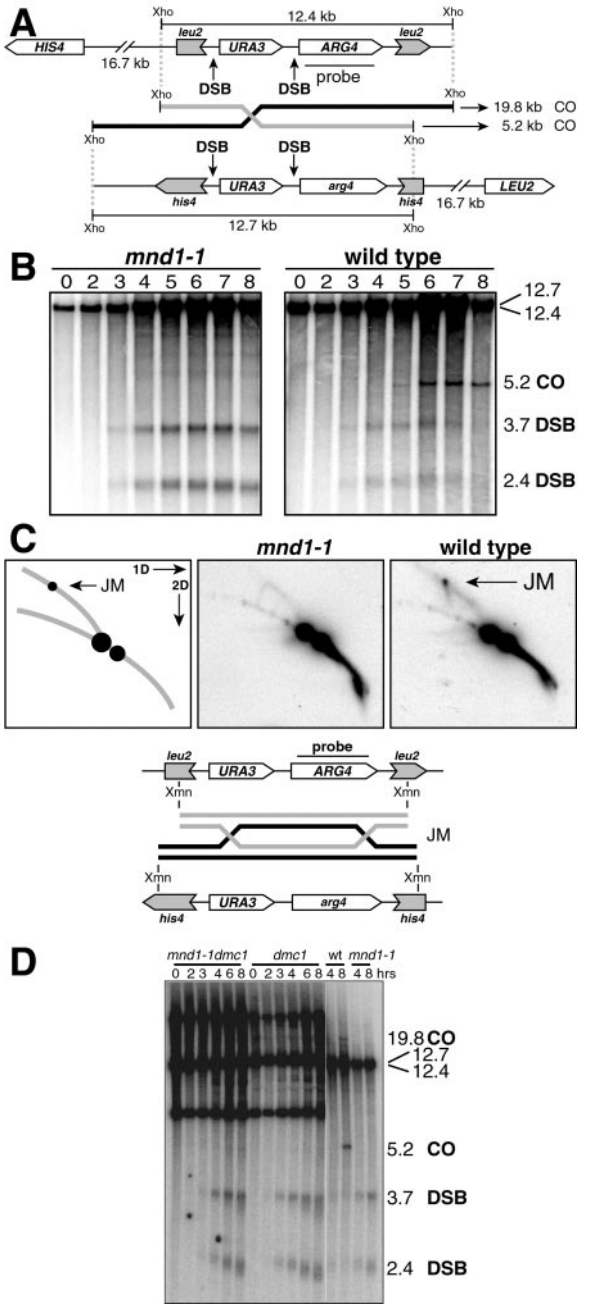

Fig. 5. Physical analysis of chromosome III, SK1. (*A*) Map of chromosome III. One homolog had a *URA3-ARG4* casette inserted into the *leu2* gene and the other homolog had the same cassette, plus a 36-bp palindrome at the *Eco*RI site in *arg4* (*his4*::*arg4-pal*), inserted into the *his4* gene. *HIS4* and *LEU2* were offset by 16.7 kb. (*B*) Genomic DNA was isolated from a sporulating culture of a wt strain (MJL2442) or *mnd1–1* strain (JG774) at the hours indicated. DNA was digested with *Xho*I, electrophoresed on a 0.5% agarose gel, transferred to a nylon membrane, and probed with a ^{32}P-labeled DNA sequence derived from *ARG4*. The parental fragments are 12.4 and 12.7 kb, the DSB fragments are 3.7 and 2.4 kb, and the CO fragments are 5.2 and 19.8 kb. (*C*) Genomic DNA was isolated from the same sporulating cultures depicted in *B* at 5 h. This DNA was digested with *XmnI* and analyzed by native/native 2D electrophoresis. DNA will migrate according to molecular weight in the first dimension and both molecular weight and shape in the second dimension. The 4- and 5-kb parental fragments migrate at their expected position, but JMs are retarded in the second dimension and migrate above the arc of linear fragments (shown in the interpretive panel). (*D*) DSBs at the *ARG4-URA3* hotspot in SK1. Genomic DNA was isolated from a sporulating culture of a wt strain (MJL2442), *mnd1–1* strain (JG774), *dmc1* strain (JG820), and *mnd1–1dmc1* strain (JG819) at the hours indicated. Analysis was carried out as in *B*.

DNA migrates in an arc pattern, but DNA with deviations in shape, such as JMs, migrates off the arc (7). We prepared genomic DNA from the aforementioned two time courses from wt and *mnd1–1* by using a protocol that preserves JMs (13). JMs could be detected in wt between 3.5 and 6 h (5 h, Fig. 5*C*) but were absent at 4, 5, 6, and 8 h in *mnd1–1* (5 h, Fig. 5*C*).

hDNA and JM formation may be impaired for at least two reasons in an *mnd1–1* strain: (*i*) the 5′ ends are not resected or (*ii*) strand invasion itself is impaired. A comparison between DSBs in *mnd1–1*, *dmc1*, *mnd1–1dmc1*, and wt strains revealed elongated smears in the case of the *dmc1* and *mnd1–1dmc1* strains, a short smear in the case of wt, and an intermediate smear in the case of *mnd1–1* (Fig. 5*D*). This result suggests that 5′ ends are resected and strand invasion is impaired in an *mnd1–1* strain. Furthermore, in an *mnd1–1dmc1* strain, the DSBs showed the same resection phenotype as in a *dmc1* strain, indicating that these two genes are epistatic for end resection.

Discussion

We have taken a functional genomics approach to identifying new genes involved in meiotic recombination. We analyzed the meiotic phenotype of null mutations in uncharacterized genes with expression profiles similar to genes known to be involved in meiotic recombination. In this way, we identified *MND1*. Like many genes in this expression cluster (see Table 1), *MND1* is spliced during meiosis. Mutation of this gene caused an arrest before the first meiotic division. The cells arrested because of the *RAD17*-mediated checkpoint, which detects unresolved recombination intermediates. *MND1* is not required for the initiation of meiotic recombination, because DSB formation is at or above wt levels at four different DSB sites. Recombination rates between heteroalleles of *arg4* and *his4* in return-to-growth experiments indicate that induction of recombination is nearly normal in an *mnd1–1* strain. However, neither hDNA nor JMs can be detected, indicating that these recombination intermediates are not present or are highly unstable. COs, a product of JMs, are undetectable. The DSB ends in an *mnd1–1* strain are slightly hyperresected compared with a wt strain, but less resected than ends in a *dmc1* strain. Based on this analysis, Mnd1p appears to be required for 3′ single-stranded ends to stably invade the homologous chromosome.

Recombination between heteroalleles in the return-to-growth assay reflects recombination events initiated during meiosis that are then resolved during vegetative growth. Our results indicate that either (*i*) a DSB is enough to stimulate heteroallele recombination and the remainder of the recombination event can be completed by using vegetative proteins or (*ii*) strand invasion is normally required for elevated recombination levels but a vegetative protein can substitute for Mnd1p.

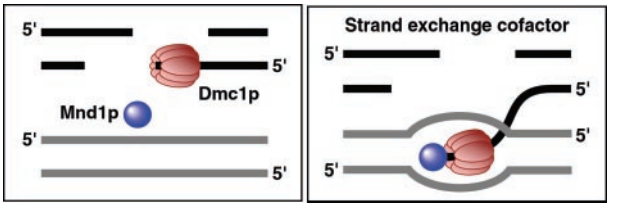

Fig. 6. Dmc1p is depicted as an oval, Mnd1p is depicted as a circle. Mnd1p may be present in multiple copies; only one is shown for illustration. Human Dmc1p forms octameric rings that can stack on DNA (36, 37); only one octamer is shown for illustration. Mnd1p could potentially be involved in one or more of the following: (*i*) disassembly of Dmc1p from single-stranded DNA, (*ii*) distortion of the unbroken homolog to facilitate invasion by the Dmc1p-associated single-stranded DNA, or (iii) efficient strand invasion/assimilation activity along with Dmc1p.

Dmc1p and Rad51p are both yeast orthologs of *Escherichia coli* RecA protein. However, these proteins appear to have distinct roles in the cell. Dmc1p shows meiosis-specific expression and the null strain displays an arrest before meiosis I (23), whereas a *rad51* strain has both mitotic and meiotic defects, and the meiotic defect is not as severe (27). Similar to *mnd1–1*, the meiosis I block in a *dmc1* strain can be bypassed by mutation of the *RAD17*-mediated checkpoint (20). A *dmc1* strain does not contain any single-end invasions (24). Based on these observations and others, both Hunter and Kleckner (24) and Shinohara *et al.* (28) have proposed that Dmc1p and Rad51p are asymmetrically located on the 3′ single-stranded tails of DSBs, and that the Dmc1p-associated end is the end that initiates strand invasion. However, eukaryotic Dmc1p is poor at promoting extensive strand exchange as measured *in vitro* (29, 30). It has thus been proposed that other proteins may be required for this reaction to occur efficiently *in vivo*. Based on the similarity in phenotype between *mnd1–1* and *dmc1* mutants, we propose that the defect in an *mnd1–1* strain is at a similar step in recombination, and furthermore, that these two proteins may act in concert *in vivo*.

Our results support a model in which Mnd1p operates downstream of Dmc1p binding to DNA (Fig. 6). DSBs in a *dmc1* strain are hyperresected, presumably because Dmc1p normally protects DNA ends from degradation by cellular nucleases. In an *mnd1–1* strain, the ends appear more protected from degradation, suggesting that Dmc1p, or a protein complex containing Dmc1p, is bound. The *dmc1mnd1–1* strain has the same phenotype as the *dmc1* strain, indicating that the defect in end protection in the double mutant strain is identical to the defect in the *dmc1* strain. In addition, Dmc1p foci are present by cytology in an *mnd1–1* strain (T. Holzen and D. Bishop, personal communication). Based on these observations, we disfavor the possibility that Mnd1p is required for Dmc1p to efficiently assemble on single-stranded DNA *in vivo*, but rather propose that Mnd1p operates downstream of Dmc1p binding to DNA. Mnd1p may be a cofactor for strand invasion.

Observing physical recombination intermediates in eukaryotes other than yeast has been difficult. Thus, the only means we have to compare recombination mechanisms across evolution is comparative genomics. With the identification of *SPO11*, *MND1*, and *DMC1* orthologs in yeasts, mouse, human, and plants, the likelihood of evolutionarily conserved recombination machinery for these organisms grows stronger. We and others have been unable to identify an ortholog of either *MND1* or *DMC1* in *D. melanogaster* or *C. elegans*. Synaptonemal complex formation also differs for these organisms; Spo11p is not required for synapsis in flies and worms (31, 32), but is required in mouse and yeast cells (33–35). These differences raise the issue as to whether flies and worms have evolved recombination mechanisms that differ substantially from those of yeast, mouse, and human.

We thank M. Lichten, I. Herskowitz, H. Madhani, D. Nag, and T. Petes for strains, oligos, and plasmids and V. Nyguen for help running 2D gels. We thank T. Holzen and D. Bishop for sharing unpublished data and helpful suggestions. For helpful discussions and comments we thank K. Benjamin, P. Brown, T. Clark, T. Petes, A. Sil, J. Brickner, and the Johnson and DeRisi labs. J.L.G. was supported by American Cancer Society Grant PF-99-017-01. J.D. was supported by a Sandler Fellowship and Howard Hughes Medical Institute Grant 5300246.

1. Keeney, S., Giroux, C. N. & Kleckner, N. (1997) *Cell* **88,** 375–384.
2. Bergerat, A., de Massy, B., Gadelle, D., Varoutas, P. C., Nicolas, A. & Forterre, P. (1997) *Nature (London)* **386,** 414–417.
3. Sun, H., Treco, D. & Szostak, J. W. (1991) *Cell* **64,** 1155–1161.
4. Schwacha, A. & Kleckner, N. (1995) *Cell* **83,** 783–791.
5. Allers, T. & Lichten, M. (2001) *Mol. Cell.* **8,** 225–231.
6. Szostak, J. W., Orr-Weaver, T. L., Rothstein, R. J. & Stahl, F. W. (1983) *Cell* **33,** 25–35.
7. Allers, T. & Lichten, M. (2001) *Cell* **106,** 47–57.
8. Rabitsch, K. P., Toth, A., Galova, M., Schleiffer, A., Schaffner, G., Aigner, E., Rupp, C., Penkner, A. M., Moreno-Borchart, A. C., Primig, M., *et al*. (2001) *Curr. Biol.* **11,** 1001–1009.
9. Smith, K. N., Penkner, A., Ohta, K., Klein, F. & Nicolas, A. (2001) *Curr. Biol.* **11,** 88–97.
10. Fan, Q., Xu, F. & Petes, T. D. (1995) *Mol. Cell. Biol.* **15,** 1679–1688.
11. Detloff, P., Sieber, J. & Petes, T. D. (1991) *Mol. Cell. Biol.* **11,** 737–745.
12. Nag, D. K. & Petes, T. D. (1993) *Mol. Cell. Biol.* **13,** 2324–2331.
13. Allers, T. & Lichten, M. (2000) *Nucleic Acids Res.*, http://nar.oupjournals.org/cgi/content/full/28/2/e6.
14. Chu, S., DeRisi, J., Eisen, M., Mulholland, J., Botstein, D., Brown, P. O. & Herskowitz, I. (1998) *Science* **282,** 699–705.
15. Maniatis, T., Fritsch, E. F. & Sambrook, J. (1989) *Molecular Cloning: A Laboratory Manual* (Cold Spring Harbor Lab. Press, Plainview, NY), 2nd Ed.
16. Knop, M. & Strasser, K. (2000) *EMBO J.* **19,** 3657–3667.
17. Blandin, G., Durrens, P., Tekaia, F., Aigle, M., Bolotin-Fukuhara, M., Bon, E., Casaregola, S., de Montigny, J., Gaillardin, C., Lepingle, A., *et al*. (2000) *FEBS Lett.* **487,** 31–36.
18. Cokol, M., Nair, R. & Rost, B. (2000) *EMBO Rep.* **1,** 411–415.
19. Klapholz, S. & Esposito, R. E. (1980) *Genetics* **96,** 589–611.
20. Lydall, D., Nikolsky, Y., Bishop, D. K. & Weinert, T. (1996) *Nature (London)* **383,** 840–843.
21. Klapholz, S., Waddell, C. S. & Esposito, R. E. (1985) *Genetics* **110,** 187–216.
22. Sherman, F. & Roman, H. (1963) *Genetics* **48,** 255–261.
23. Bishop, D. K., Park, D., Xu, L. & Kleckner, N. (1992) *Cell* **69,** 439–456.
24. Hunter, N. & Kleckner, N. (2001) *Cell* **106,** 59–70.
25. Detloff, P. & Petes, T. D. (1992) *Mol. Cell. Biol.* **12,** 1805–1814.
26. Alani, E., Padmore, R. & Kleckner, N. (1990) *Cell* **61,** 419–436.
27. Shinohara, A., Ogawa, H. & Ogawa, T. (1992) *Cell* **69,** 457–470.
28. Shinohara, M., Gasior, S. L., Bishop, D. K. & Shinohara, A. (2000) *Proc. Natl. Acad. Sci. USA* **97,** 10814–10819.
29. Hong, E. L., Shinohara, A. & Bishop, D. K. (2001) *J. Biol. Chem.* **276,** 41906–41912.
30. Masson, J. Y. & West, S. C. (2001) *Trends Biochem. Sci.* **26,** 131–136.
31. McKim, K. S., Green-Marroquin, B. L., Sekelsky, J. J., Chin, G., Steinberg, C., Khodosh, R. & Hawley, R. S. (1998) *Science* **279,** 876–878.
32. Dernburg, A. F., McDonald, K., Moulder, G., Barstead, R., Dresser, M. & Villeneuve, A. M. (1998) *Cell* **94,** 387–398.
33. Romanienko, P. J. & Camerini-Otero, R. D. (2000) *Mol. Cell.* **6,** 975–987.
34. Baudat, F., Manova, K., Yuen, J. P., Jasin, M. & Keeney, S. (2000) *Mol. Cell.* **6,** 989–998.
35. Cha, R. S., Weiner, B. M., Keeney, S., Dekker, J. & Kleckner, N. (2000) *Genes Dev.* **14,** 493–503.
36. Masson, J. Y., Davies, A. A., Hajibagheri, N., Van Dyck, E., Benson, F. E., Stasiak, A. Z., Stasiak, A. & West, S. C. (1999) *EMBO J.* **18,** 6552–6560.
37. Passy, S. I., Yu, X., Li, Z., Radding, C. M., Masson, J. Y., West, S. C. & Egelman, E. H. (1999) *Proc. Natl. Acad. Sci. USA* **96,** 10684–10688.